Synthesis, Structure, and Chemical Properties of Lithium Salts of Poly(2-methoxyaniline-5-sulfonic acid)

Takakazu Yamamoto,*,† Asako Ushiro,† Isao Yamaguchi,† and Shintaro Sasaki‡

Chemical Resources Laboratory, Tokyo Institute of Technology, 4259 Nagatsuta, Midori-ku, Yokohama 226-8503, Japan, and Japan Advanced Institute of Science and Technology, 1-1 Asahidai, Tatsunokuchi, Ishikawa 923-1292, Japan

Received June 21, 2002; Revised Manuscript Received February 7, 2003

ABSTRACT: Treatment of poly(2-methoxyaniline-5-sulfonic acid) (**PAS**) with LiOH gave its lithium salts, **PAS(Li)**s, with various degrees of lithium sulfonation. Structure of a fully lithium-sulfonated **PAS(Li)** was determined by ^{1}H NMR spectroscopy and elemental analysis. Cyclic voltammetry and complex impedance analysis revealed electrochemical properties of the **PAS(Li)** films depending on the degree of the lithium sulfonation. **PAS(Li)**s had ionic conductivity of about 1×10^{-6} S cm^{-1} at 302 K. The packing structure of **PAS(Li)** is discussed on the basis of powder XRD data.

Introduction

Sulfonated polyanilines (SPANs) have attracted interest due to their unique electrochemical properties, improved processability, and potential industrial applications.[1] Recently, various SPANs have been synthesized by oxidative,[2] electrochemical,[3] and enzymatic[4] polymerizations and graft reactions on amine nitrogen.[5,6] Application of SPANs as useful materials for rechargeable batteries,[7] light-emitting diodes,[8−10] and patterning on a wafer[11] has also been developed owing to their self-doping behavior to show high electrical conductivity and intriguing optical properties. Self-doping behavior of sulfonated π-conjugated conducting polymers is the subject of recent interest.[1,12]

The sulfonic acid proton in SPAN is considered to play an important role in the self-doping. Thus, substitution of the sulfonic acid proton in SPAN with other ions such as alkaline metal will alter its chemical properties. Epstein and MacDiarmid reported optical and chemical data of SPAN and alkaline metal salts of SPAN in their effort to reveal the self-doping behavior of SPAN.[1] However, revealing other chemical properties of SPAN and its alkaline-metal salts will still be of interest.

Solid polymer electrolytes for lithium batteries have recently attracted attention. Substitution of the sulfonic acid proton in SPAN with a lithium ion will provide a new lithium ion conductor.[13] Since the anionic part, $-SO_3^-$, is fixed in the polymer matrix, ionic conduction of this type of lithium ion conductor will be attributed to movement of Li^+ in the solid. Examples of such a "single-ion" type solid lithium conductor have been limited. We herein report lithium sulfonation of poly(2-methoxyaniline-5-sulfonic acid) (**PAS**) and isolation of its lithium salts, **PAS(Li)**s. Structures, optical properties, and ionic conductivity of **PAS(Li)**s are also reported. Because of the presence of the OCH_3 group, solubility of the polymer is increased compared with nonsubstituted SPAN, and the OCH_3 group is expected to afford additional information for the polymer, e.g., by ^{1}H NMR spectroscopy.

† Tokyo Institute of Technology.
‡ Japan Advanced Institute of Science and Technology.

Scheme 1. Structure of PAS

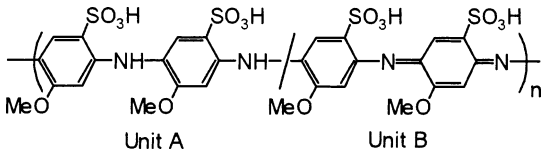

Experimental Section

Materials and Measurements. Poly(2-methoxyaniline-5-sulfonic acid), **PAS**,[1i,j] and poly(aniline sulfonic acid), SPAN, were kindly presented by Mitsubishi Rayon Co. Other chemicals including buffer solutions (pH = 1, KCl−HCl; pH = 4, C_6H_4(COOK)(COOH); pH = 7, KH_2PO_4−NaOH; pH = 10, $NaHCO_3$−NaOH) were used as purchased. Elemental and induced plasma coupling (ICP) analyses were carried out on a Yanagimoto Type MT-2 CHN autocorder and a Seiko Electron SPS1500VR, respectively. ^{1}H NMR spectra were recorded on a JEOL EX-400 spectrometer. UV−vis. spectra and X-ray diffraction patterns were obtained by a Shimadzu UV-2100PC spectrometer and a Philips PS-1051 or Rigaku RAXIS−IIc X-ray diffractometers, respectively. Cyclic voltammetry was performed in an acetonitrile solution containing 0.10 M $[Et_4N]BF_4$ with a Solartron SI 1287 electrochemical interface. Cole−Cole plots were recorded on a Solartron SI 1287 electrochemical interface/gain-phase analyzer. Samples (pressed sheets) for the complex impedance analysis were sandwiched between round stainless steel electrodes (diameter = 1.33 cm), pumped under vacuum at 100 °C for 24 h, and sealed under inert gas atmosphere after cooled to room temperature. Certain data for ionic conductivity were kindly measured at Yuasa Corp., and supporting data were taken in our laboratory.

Preparation of Lithium Salts of PAS. To an aqueous solution (10 mL) of poly(2-methoxyaniline-5-sulfonic acid) (**PAS**) (0.50 g, 2.5 mmol aniline unit) was added 4 mL of LiOH (aq) (0.63 M, 2.5 mmol). After being stirred at room temperature for 2.5 h, the reaction mixture was poured into THF (200 mL) to obtain a precipitate, which was collected by filtration and dried under vacuum to yield **PAS(Li)-4** (0.37 g, 68%). Anal. Calcd for (Li salt of unit A)$_{0.95}$(Li salt of unit B)$_{0.95}$(unit A)$_{0.05}$(unit B)$_{0.05}$·4.5H_2O or $(C_7H_6NSO_4Li)_{0.95}(C_7H_5NSO_4Li)_{0.95}$-$(C_7H_7NSO_4)_{0.05}(C_7H_6NSO_4)_{0.05}$·4.5$H_2O$: C, 34.06; H, 4.10; N, 5.67; O, 40.51. Found: C, 34.51; H, 4.51; N, 5.90; O, 40.70. ICP analysis of Li agreed with the formulation of the product. **PAS(Li)-1**, **-2**, and **-3** were prepared analogously by adding 0.1, 0.5, and 0.7 mol of LiOH per aniline unit of **PAS**, respectively. ICP analysis of Li of **PAS(Li)-1**, **-2**, and **-3** indicated that their degrees of the lithiation were 8, 46, and 64%, respectively.

10.1021/ma0209747 CCC: $25.00
Published on Web 08/16/2003

Leucoemeraldine type **PAS**, **LE-PAS**, was prepared by reaction of powdery **PAS** (180 mg, 0.88 mmol aniline unit) with hydrazine hydrate (8.0 mL; excess) at room temperature for 45 h. After removal of hydrazine hydrate, the obtained reddish gray powder of **LE-PAS** was dried under vacuum. 1:1 reaction of **LE-PAS** with LiOH gave **LE-PAS(Li)**: yield = 69%.

Results and Discussion

Preparation of PAS(Li) and IR and NMR Analysis. Treatment of poly(2-methoxyaniline-5-sulfonic acid) (**PAS**) with LiOH in 1:0.1, 1:0.5, 1:0.7, and 1:1 molar ratios in water gave lithium salts of **PAS** (**PAS(Li)-1** through **PAS(Li)-4**) in 68−83% yields (eq 1). **PAS(Li)-1** through **PAS(Li)-4** were hygroscopic and stored under inert gas.

PAS + LiOH $\xrightarrow[H_2O]{}$ **PAS(Li)** (1)

		degree of lithiation (ICP)
1 : 0.1	**PAS(Li)-1**	8%
1 : 0.5	**PAS(Li)-2**	46%
1 : 0.7	**PAS(Li)-3**	64%
1 : 1	**PAS(Li)-4**	95%

Induced plasma coupling (ICP) analysis showed that degrees of lithium sulfonation of **PAS(Li)-1**-**PAS(Li)-4** were 8, 46, 64, and 95%, respectively, indicating that the lithium sulfonation proceeded effectively. Lithiation of **PAS** with LiH (excess) under heterogeneous conditions in diethyl ether also proceeded, and its ^{1}H NMR spectrum (vide infra) resembled that of **PAS(Li)-3**.

For comparison and NMR characterization, a similar reaction of the leucoemeraldine base of poly(2-methoxyaniline-5-sulfonic acid) (**LE-PAS**), which was prepared by treatment of **PAS** with hydrazine monohydrate, with LiOH was carried out in a 1:1 molar ratio to provide **LE-PAS(Li)** in 69% yield (eq 2); reduction of emeraldine base type polyanilines with hydrazine monohydrate has been reported.[1e]

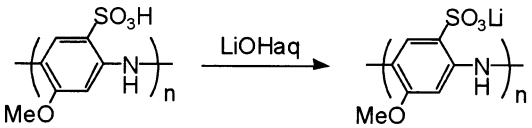

LE-PAS **LE-PAS(Li)** (2)

IR spectra of **PAS**, **PAS(Li)s**, **LE-PAS**, and **LE-PAS-(Li)** resemble each other, as explained in Figure 1. They show aromatic skeletal and C−N peaks at about 1620 and 1540 cm^{-1} and peaks at 1220 and 1080 cm^{-1} which are assigned to ν_{asym}(C−O−C) and ν_{sym}(C−O−C), respectively, by comparing the IR spectrum with that of SPAN without the OCH_3 group.[1h] The aliphatic ν(C−H) peak of the OCH_3 group of **LE-PAS** is observable at about 2940 cm^{-1}. However, the aliphatic peak is not observable with other samples. It was reported that generation of oxidized (or p-doped) state in conducting polymers gave severe electronic effect on alkoxy and alkyl substituents to decrease the IR and ^{1}H NMR intensity.[14]

Figure 2 depicts ^{1}H NMR spectra of (a) **LE-PAS(Li)** and (b) **PAS(Li)-4** in DMSO-d_6. As shown in Figure 1a, **LE-PAS(Li)** gives peaks due to benzenoide hydrogens at δ 6.62 and 7.62 in an equal intensity. A peak at δ 7.96 is assigned to the NH hydrogen. Observed peak area ratio of the NH peak to that of the aromatic H peak (1:2.2) agreed with the molecular structure of **LE-PAS-(Li)** within experimental error. The NH peak intensity decreased profoundly on addition of a small amount D_2O, supporting the assignment of the NH signal. Appearance of the NH peak of polyanilines at about δ 8 has been reported.[15]

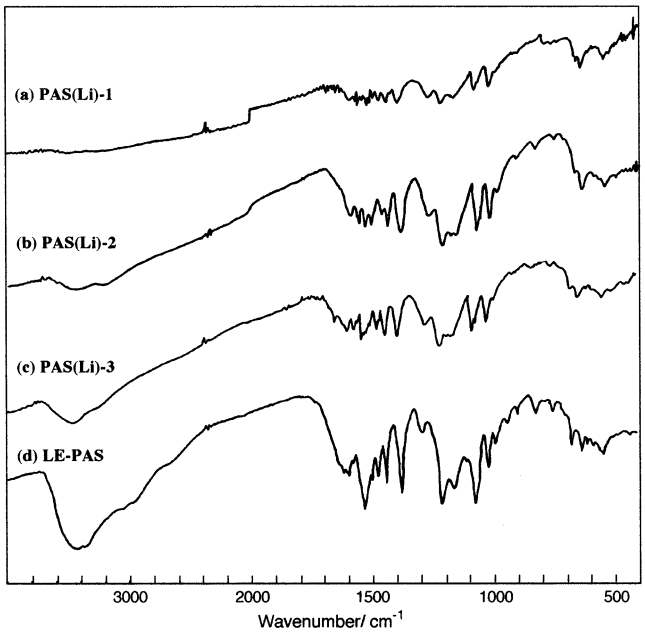

Figure 1. IR spectra of **PAS(Li)-1**, **PAS(Li)-2**, **PAS(Li)-3**, and **LE-PAS**.

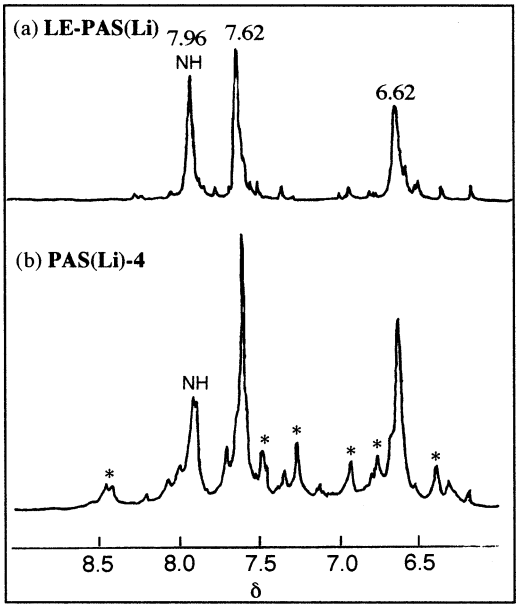

Figure 2. ^{1}H NMR spectra of (a) **LE-PAS(Li)** and (b) **PASLi-4** in DMSO-d_6.

As shown in Figure 2b, the NH peak is weakened for **PAS(Li)-4**. Since emeraldine base type polymer contains various types of aromatic hydrogens, the ^{1}H NMR spectrum of **PAS(Li)-4** becomes complicated and exhibits many new peaks. If all of the new peaks (peaks marked with an asterisk in Figure 2b), including the peak at about δ 8.4, are assigned to the aromatic hydrogens, the peak area ratio of the NH peak to that of total aromatic H peaks (1:4.0) agrees with the structure of the emeraldine type polymer. However, for **PAS(Li)-4**, addition of a small amount of D_2O did not decrease the NH peak intensity, indicating that the H exchange reaction did not proceed well under the

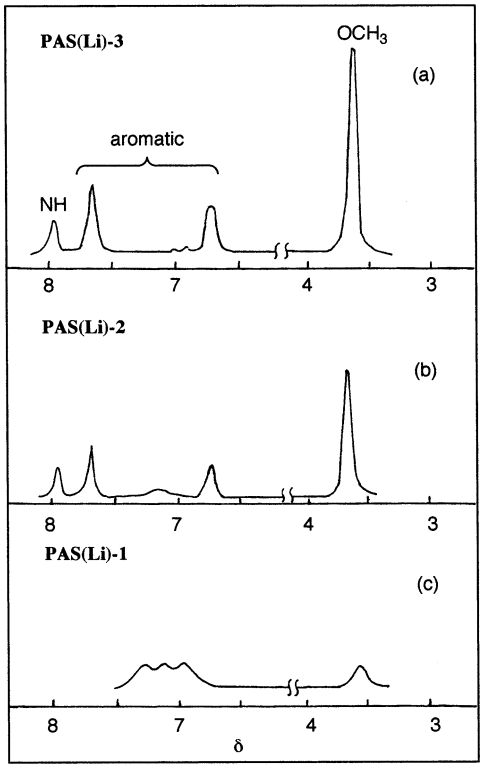

Figure 3. ^{1}H NMR spectra of (a) **PAS(Li)-3**, (b) **PAS(Li)-2**, and (c) **PAS(Li)-1** in DMSO-d_6.

alkaline conditions. The OCH_3 peak of **LE-PAS(Li)** and **PAS(Li)-4** appears at about δ 3.7 with reasonable intensity.

Figure 3 exhibits ^{1}H NMR spectra of **PAS(Li)-1** through **PAS(Li)-3**. The ^{1}H NMR spectrum **PAS(Li)-3** (chart a in Figure 3) differs from that of **PAS(Li)-4**, and resembles that of **LE-PAS(Li)** although the intensity of the NH peak is reasonably weaker for **PAS(Li)-3**. The simple peak pattern of the aromatic protons, compared with that of **PAS(Li)-4**, suggests rapid exchange of Li around various $-SO_3^-$ or $-SO_3H$ sites in **PAS(Li)-3**. **PAS(Li)-2** also gives the NH, aromatic $-$H, and OCH_3 signals at almost the same positions. However, the intensity of the OCH_3 signal is somewhat decreased (to about 70% of normal). A new broad peak at about δ 7.1 may be assigned to hydrated water.[16] For **PAS(Li)-1**, the OCH_3 signal is strongly weakened. Such weakening of the OR peak on p-doping of the conducting polymer has been reported with poly(3-methoxythiophene)[14a,c] and poly(ethylenedioxythiophene)s[14c] and elucidated by generation of a special magnetic state at the OR group according to a shift of one of the lone pair electrons to the positively charged main chain; e.g.

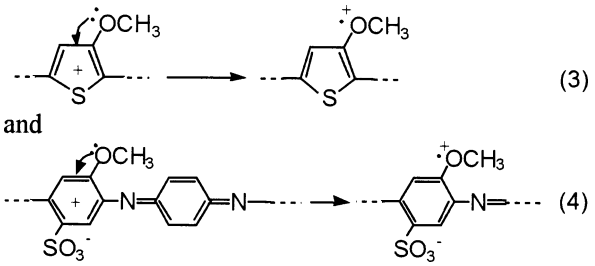

Such a type of electron shift is conceivable for **PAS-(Li)-1**, and this may also be the reason for weakening of the OCH_3 signal. On the other hand, for **PAS(Li)-4** and **PAS(Li)-3**, self-doping to generate the positive change in the main chain will proceed to only a minor extent, and the OCH_3 signal appears normally. ^{1}H NMR spectrum of **PAS** itself showed a peak pattern similar to that of **PAS(Li)-1** for a range of δ 6.5$-$8, and the OCH_3 peak was not detected with **PAS**.

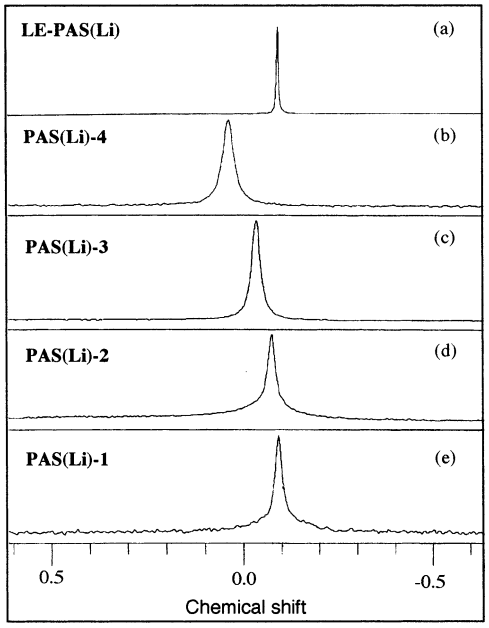

Figure 4. ^{7}Li NMR spectra of (a) **LE-PAS(Li)**, (b) **PAS(Li)-4**, (c) **PAS(Li)-3**, (d) **PAS(Li)-2**, and (e) **PAS(Li)-1** in DMSO-d_6. Chemical shift (in ppm) is referred to external LiCl in DMSO-d_6. 1 ppm = 194 Hz. At 50 °C.

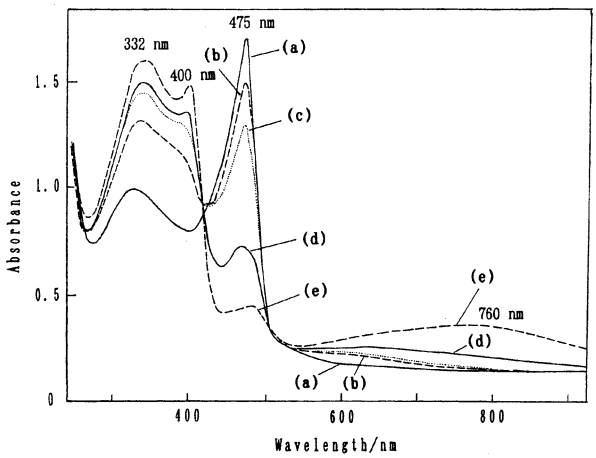

Figure 5. Change of UV$-$vis spectra of **PAS** on addition of LiOH. In water at 25 °C. [aniline unit of PAS] = 2.7×10^{-4} M. [LiOH]/[aniline unit]: (a) 0 (—); (b) 0.41 (- - -); (c) 0.67 (···); (d) 1.7 (—); (e) 5.4 (- - -).

Figure 4 shows ^{7}Li NMR spectra of the Li salts referred to LiCl in DMSO-d_6. Since the peak position locates near that of LiCl, which is considered to dissociate in DMSO,[17] the $-SO_3Li$ group in **LE-PAS(Li)** and **PAS(Li)-1** through **PAS(Li)-4** is considered to be essentially dissociated. The signal of **LE-PAS(Li)** is sharp enough. However, peaks of other samples are somewhat broadened, suggesting the presence of a kinetic exchange process between various chemical species.

UV$-$Vis Data. Curve a in Figure 5 shows the UV$-$vis spectrum of **PAS** in H_2O. The peaks at 475 and about 330 nm are compared with those at 566 and 320 nm of SPAN base measured in aqueous 0.1 M NH_4OH.[1h]

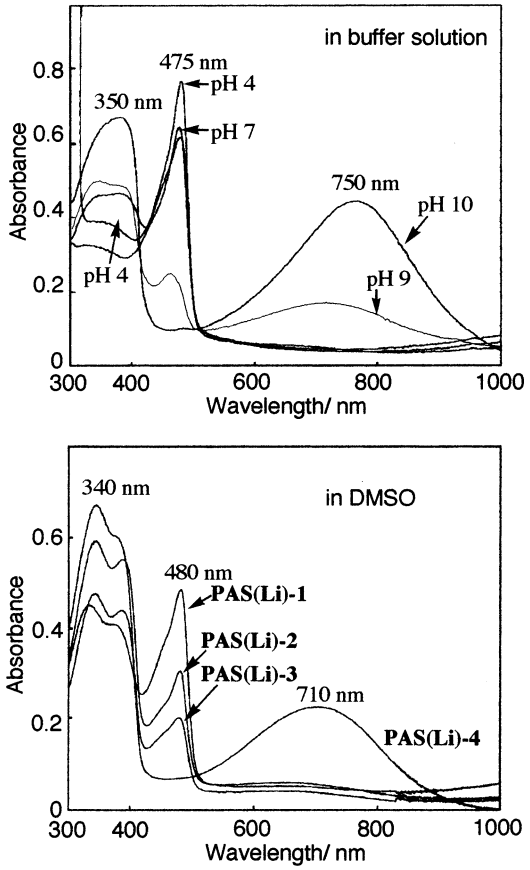

Figure 6. Top: UV−vis spectra of **PAS** in various aqueous buffer solutions. At pH = 13, a spectrum similar to that observed at pH = 10 was obtained. Bottom: UV−vis spectra of **PAS(Li)-1** through **-4** in DMSO.

The two peaks of SPAN were assigned to exciton transition and benzonoid $\pi-\pi^*$ transition, respectively.[1h,18,19]

On addition of LiOH to the solution of **PAS**, the peak at 475 nm decreases and the peak at about 330 nm increases, which is accompanied by the appearance of a new peak at about 400 nm. The decrease of the peak at 475 nm is associated with decrease in the degree of the self-doping or decrease in the positively charged main chain which is led by the $-SO_3H$ group (not by the $-SO_3Li$ group). Further addition of LiOH caused appearance of a new broad peak at about 760 nm, as shown by curve e in Figure 5. It was previously reported that alkaline metal salts of SPAN also gave a new peak in this region.[1a] Observation of the absorption peak at a longer wavelength was also reported for the UV−vis spectrum of emeraldine base type polyaniline doped with LiCl.[20]

The data shown in the top figure of Figure 6 measured in buffer solutions reveal that the new peak starts to appear at about pH = 9, where the replacement of the $-SO_3H$ hydrogen with alkaline metal proceeds extensively. The UV−vis data of **PAS(Li)-1** through **PAS-(Li)-4** (Figure 6, bottom) also supports this view that the new peak is characteristic of highly lithiated **PAS**. The titration curve of **PAS** depicted in Figure 7 indicates that neutralization of **PAS** proceeds normally; organic sulfonic acids have pK_a values of about 4, and the acidity of polymeric acids usually becomes weaker as the titration proceeds.

Viscosity. As shown in Figure 8, the η_{sp}/c value of **PAS** and **PAS(Li)-3** increases when the concentration

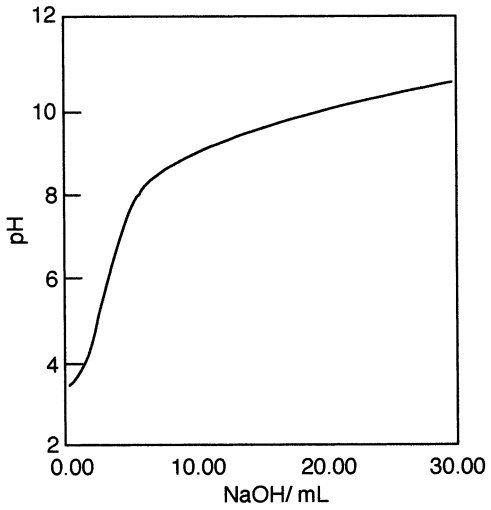

Figure 7. Titration curve of **PAS**. An aqueous solution NaOH (7.08×10^{-3} M) was added to an aqueous solution (20 mL) of **PAS** (10.2×10^{-3} M of the monomeric unit); 28.8 mL of the NaOH solution corresponds to the 1:1 molar ratio. At 24 °C.

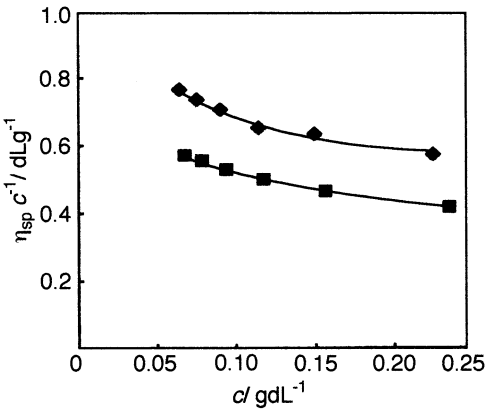

Figure 8. η_{sp}/c vs c plots for **PAS** (■) and **PAS(Li)-3** (◆) in H_2O at 30 °C.

c is decreased, in accord with the expected behavior of polymeric electrolytes.[21] Fuoss's plots[21b] of data shown in Figure gave [η] values of 1.01 and 1.22 dL g^{-1} for **PAS** and **PAS(Li)-3**. These data suggest that **PAS-(Li)-3** takes a stiffer structure than **PAS** in the aqueous solution.

Cyclic Voltammetry (CV). Cast film of **PAS** on a Pt plate received two step electrochemical oxidation with the first peak anode potential $E_{pa}(1)$ and the second peak anode potential $E_{pa}(2)$ at −0.06 and 0.64 V vs Ag^+/Ag, respectively, in an acetonitrile solution of 0.10 M $[NEt]_4BF_4$. The anode potentials were somewhat lower than those observed in HCl(aq).[1b] The two oxidation peaks were coupled with cathodic peaks, $E_{pc}(1)$ and $E_{pc}(2)$, at −0.28 and 0.34 V vs Ag^+/Ag, respectively. During the two step oxidation, about 0.5 positive charge was stored per the repeating monomeric unit. According to the lithiation, the peak potentials, $E_{pa}(1)$ through $E_{pc}(2)$, of **PAS(Li)**s shifted as summarized in Table 1. For **PAS** and **PAS(Li)**s, the green polymer film changed to blue after the electrochemical oxidation (or p-doping) and returned to green after passing the $E_{pc}(2)$ peak (or depoing peak). Such electrochromism has been observed with polymers containing π-conjugated systems.

Function as a Polymer Solid Electrolyte. Figure 9 exhibits time dependence of dc current observed with a **PAS(Li)-3** film under applying a constant voltage of

Table 1. Electrochemical Data for the Film of Polymers

	peak potential[a]/V			
	p-doping		p-undoping	
polymer	$E_{pa}(1)$	$E_{pa}(2)$	$E_{pc}(1)$	$E_{pc}(2)$
PAS	−0.06	0.64	−0.28	0.34
PAS(Li)-2	−0.12	0.54	−0.26	0.34
PAS(Li)-3	−0.13	0.57	−0.27	0.38
PAS(Li)-4	−0.15[b]	0.41[b]	−0.25[b]	0.21[b]

[a] Versus Ag^+/Ag. Measured in an acetnitrile solution of $[Et_4N]BF_4$ (0.1 M). [b] At first scan.

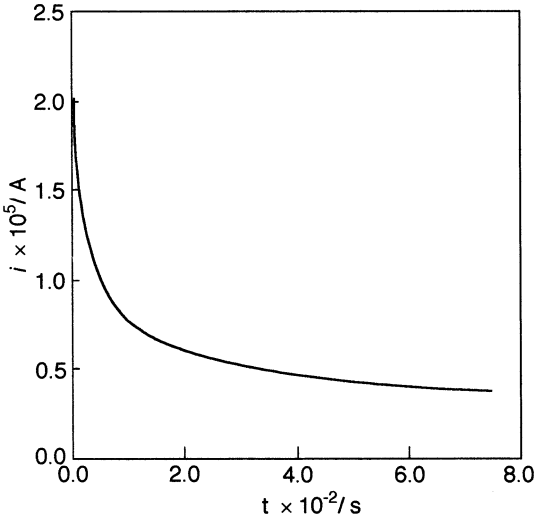

Figure 9. Time dependence of dc current for a **PAS(Li)-3** film under applying a constant voltage (50 mV) at room temperature. The polymer film was sandwiched with stainless steel plates (blocking electrodes).

50 mV. As previously reported a film of **PAS** shows dc conductivity of 4×10^{-2} S cm^{-1};[1i] other SPANs show similar electrical conductivity.[22,23] However, the sharp decrease in the dc current observed with the **PAS(Li)-3** film indicates that the electrical conductivity of **PAS(Li)-3** is mainly attributed to ionic conduction.[24] The dc current increased on raising temperature, which was ascribed to the increase in mobility of Li^+ at higher temperature and supported a view that the dc current did not originate from capacitive charging. Polymer solid electrolytes including those based on matrix polymers with high T_g[24e] have been the subject of many papers,[24] and electrical conductivity of polymer solid electrolytes is usually obtained by complex impedance analysis.

Figure 10 shows a complex impedance plot (or a so-called Cole−Cole plot) for a **PAS(Li)-3** film. In the complex impedance plot, the distance across of the arc, which is obtained under ac bias conditions, is considered to correspond to the electric resistance of the sample.[24] From the data shown in Figure 10, electrical conductivity (σ) of **PAS(Li)-3** is evaluated as 1.2×10^{-6} S cm^{-1} at 302 K. The inset in Figure 10 depicts a temperature dependence of the σ value of the film, which obeys an Ahrrenius-type equation; $\sigma = \sigma_0 \exp(-E_a/RT)$, where E_a and T are activation energy and temperature, respectively. The E_a value calculated from the slope of the linear line is 73 kJ mol^{-1}.

PAS(Li)-2 gave electrical conductivity of 1.3×10^{-6} S cm^{-1} at 311 K and an activation energy of 31 kJ mol^{-1} as evaluated from the complex impedance analysis. However, **PAS(Li)-4** showed too low electrical conductivity to measure with our apparatus (cf. Experimental

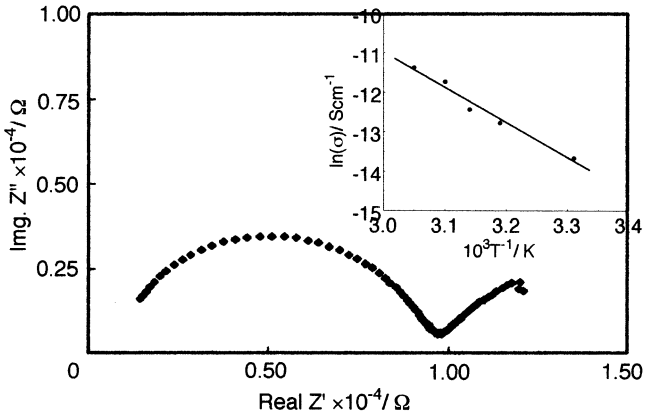

Figure 10. Complex impedance plot (Cole−Cole plot) for the **PAS(Li)-3** film at 302 K. Inset: Arrhenius plot of the electrical conductivity.

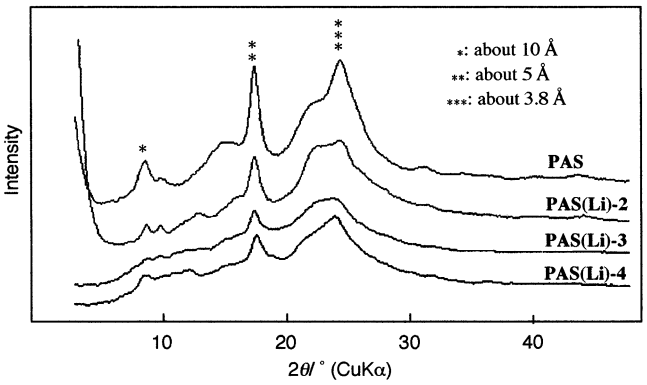

Figure 11. Powder X-ray diffraction patterns of **PAS** and **PAS(Li)-2** through **PAS(Li)-4**. The packing model based on the molecular model, model 1, explained well the features of the observed XRD curves (cf. Supporting Information).

Section). It seems difficult for the Li^+ ion to move in the fully lithiated **PAS(Li)-4**, and the presence of accepting (e.g., the $-SO_3H$ group or the $-SO_3^-$ group) site(s) for the Li^+ ion may be crucial for the ionic conduction. For various LiX−polymer (X = ClO_4, etc.; polymer is, e.g., poly(ethylene oxide)) solid electrolytes, it was reported that the ionic conductivity reaches a maximum at a particular concentration of LiX (e.g., at 1:4 molar ratio of LiX to the $-CH_2CH_2O-$ unit of poly(ethylene oxide).[24] For the usual polymer solid electrolyte, the ionic conductivity is attributed to movement of the Li^+ ion and X^- ion; however, for the present case, the X^- group ($-SO_3^-$ group) is supported in the polymer matrix and the ionic conduction is considered to originate primarily from movement of Li^+ in the polymer sample.

Electrical current of the film of **PAS(Li)-1** did not changed with time when the constant potential was applied to the film, indicating that the electrical conductivity of **PAS(Li)-1** was assigned to electronic conduction, which presumably arised from the self-doped part(s). The dc conductivity of **PAS(Li)-1** was 1.4×10^{-4} S cm^{-1} at 20 °C, which was lower than that of **PAS** (0.02 S cm^{-1}) presumably due to the decrease in the proportion of the self-doped part.

Packing Structure. Figure 11 depicts powder X-ray diffraction (XRD) patterns of **PAS**, **PAS(Li)-2**, **PAS(Li)-3**, and **PAS(Li)-4**. XRD patterns of **PAS** and **PAS(Li)-2** through **PAS(Li)-4** resembled each other, showing major peaks at 2θ (Cu Kα) = 17.5° (d = 5.1 Å) and

Chart 1. Molecular Model (Model 1) of the Repeating Unit of PAS[a]

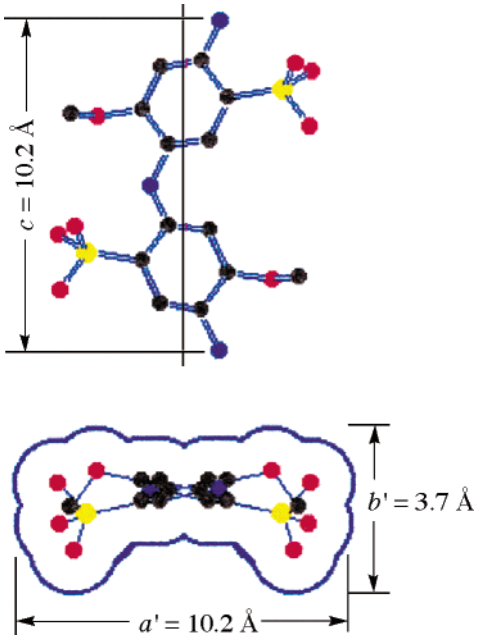

[a] Bottom: side view of the molecular model.

24.5° (d = 3.65 Å). Although various types of alkaline metal salts of polymer acids have been prepared, such isomorphorism between the mother polymer and the metal salts has no precedent to our knowledge.

MM2 calculation of the repeating unit of **PAS** gave the following molecular model. The idealized molecular model 1 in Chart 1 has a glide plane symmetry (mirror plane combined with the translation of $c/2$ along the chain axis), which arises from rotation of the aromatic ring about their para-axis.

PAS may take a molecular packing similar to that of polyaniline,[25] where the polymer molecule is considered to assume a linear (nonfolded) structure. To confirm this molecular structure, XRD patterns were calculated by the Rietveld simulation technique[26] for several orthorhombic packing models. The XRD curves calculated for a primitive unit cell with $a \doteqdot a'$ and $b \doteqdot b'$ (for a' and b', cf. model 1) and a face-centered unit cell with $a \doteqdot a'$ and $b \doteqdot b'$ agreed well with the observed one. Both packing models explained the major peaks commonly, and they could not be discriminated. The XRD curve of **PAS** calculated for the face-centered unit cell is given and compared with the observed curve in the Supporting Information. The packing structure is probably disordered to some extent. The reflections at $2\theta = 8.6°$ (d = 10.2 Å) and 24.5° (d = 3.65 Å) were attributed to the lateral periodicities of a' and b' respectively, while the 17.5° (d = 5.1 Å) reflection was assigned to the $c/2$ axial repeat (namely, 002 spacing). It is noteworthy that the Lorentz-corrected intensity of the 24.5° reflection is extraordinary strong, suggesting the face-to-face type packing of the polymer molecules. From the integral widths of the reflections at $2\theta = 8.6$ and 17.5° (1.3 and 0.9°, respectively), the lateral and the axial correlation lengths were estimated by Scherrer's equation to be about 7 and 10 nm, respectively.

Conclusion

Lithium salts of emeraldine base type and leucoemeraldine base type poly(2-methoxyaniline-5-sulfonic acid)s with various degrees of lithium sulfonation were obtained. Analytical data, including ^{1}H NMR data, revealed their structures. Electrochemical properties of **PAS(Li)** depending on the degree of the lithium sulfonation have also been revealed. **PAS** and **PAS(Li)**s showed isomorphorism in the XRD analysis.

Acknowledgment. We are gratefully to Prof. T. Kanbara in our laboratory and Mr. K. Kuwana and Mr. T. Bandou, and Dr. Y. Aihara of Yuasa Corp. for helpful discussion and experimental support. Thanks are due to donation of **PAS** and SPAN from Mitsubishi Rayon Co.

Supporting Information Available: A figure showng the comparison of the simulated XRD curve and observed XRD curve. This material is available free of charge via the Internet at http://pubs.acs.org.

References and Notes

(1) (a) Yue, J.; Epstein, A. J. *J. Am. Chem. Soc.* **1990**, *112*, 2800. (b) Yue, J.; Wang, Z. H.; Cromack, K. R.; Epstein, A. J.; MacDiarmid, A. G. *J. Am. Chem. Soc.* **1991**, *113*, 2665. (c) Yue, J.; Epstein, A. J.; Zhong, Z.; Gallagher, P. K.; MacDiarmid, A. G. *Synth. Met.* **1991**, *41*, 765. (d) Yue, J.; Gordon, G.; Epstein, A. J. *Polymer* **1992**, *33*, 4409. (e) Moon, D.-K.; Ezuka, M.; Muruyama, T.; Osakada, K.; Yamamoto, T. *Macromolecules* **1993**, *26*, 364. (f) Chen, S.-A.; Hwang, G.-W. *J. Am. Chem. Soc.* **1995**, *117*, 10055. (g) Chen, S.-A.; Hwang, G.-W. *Macromolecules* **1996**, *29*, 3950. (h) Wei, X.-L.; Wang, Y. Z.; Long, S. M.; Bobeczko, C.; Epstein, A. J. *J. Am. Chem. Soc.* **1996**, *118*, 2545. (i) Shimizu, S.; Saitoh, T.; Uzawa, M.; Yuasa, M.; Yano, K.; Maruyama, T.; Watanabe, K. *Synth. Met.* **1997**, *85*, 1337. (j) Varela, H.; Maranhaõ, S. L. de A.; Mello, R. M. Q.; Ticianelli, E. A.; Torresi, R. M. *Synth. Met.* **2001**, *122*, 321. (k) Lee, W.-P.; Brenneman, K. R.; Hsu, C.-H.; Shih, H.; Epstein, A. J. *Macromolecules* **2001**, *34*, 2648.

(2) Ohno, N.; Wang, H.-J.; Yan, H.; Toshima, N. *Polym. J.* **2001**, *33*, 165.

(3) (a) Guo, R.; Barisci, J. N.; Innis, P. C.; Too, C. O.; Wallace, G. G.; Zhou, D. *Synth. Met.* **2000**, *114*, 267. (b) Krishnamoorthy, K.; Contractor, A. Q.; Kumar, A. *Chem. Commun.* **2002**, 240.

(4) Tatsuma, T.; Ogawa, T.; Sato, R.; Oyama, N. *J. Electroanal. Chem.*, **2001**, *501*, 180.

(5) Lin, H.-K.; Chen, S.-A. *Macromolecules* **2000**, *33*, 8117.

(6) Hua, M.-Y.; Su, Y.-N.; Chen, S.-A. *Polymer* **2000**, *41*, 813.

(7) (a) Barbero, C.; Miras, M. C.; Koetz,; Haas, O. *Synth. Met.* **1993**, *55*, 1539. (b) Barbero, C.; Miras, M. C.; Schnyder, B.; Haas, O.; Koetz, R. *J. Mater. Chem.* **1994**, *4*, 1775.

(8) (a) Onoda, M.; Yoshino, K. *J. Appl. Phys.* **1995**, *78*, 4456. (b) Onoda, M.; Yoshino, K. *Jpn. J. Appl. Phys., Part 2* **1995**, *34* (2B), L260.

(9) Ferreira, M.; Rubner, M. F. *Macromolecules* **1995**, *28*, 7107.

(10) Sun, J.; Sun, J.; Ma, Y.; Zhang, X.; Shen, J. *Mater. Sci. Eng.* **1999**, *C10*, 83.

(11) Namiki, T.; Yano, E.; Watabe, K.; Igarashi, Y.; Kuramitsu, Y.; Maruyama, T.; Yano, K.; Nakamura, T.; Shimizu, S.; Saito, T. Patent, JP07179754.

(12) (a) Patil, A. O.; Ikenoue, F. I.; Wudl, F.; Heeger, A. J. *J. Am. Chem. Soc.* **1987**, *109*, 1858. (b) Chen, S.-A.; Hwang, G.-W. *J. Am. Chem. Soc.* **1994**, *116*, 7939. (c) Chan, H. S. O.; Ho, P. K. H.; Ng, S. C.; Tan, B. T. G.; Tan, K. L. *J. Am. Chem. Soc.* **1995**, *117*, 8517. (d) Yamamoto, T.; Shimizu, T.; Kurokawa, E. *React. Funct. Polym.* **2000**, *43*, 79. (e) Yamamoto, T.; Sakamaki, M.; Fukumoto, H. *Synth. Met.* **2003**, *139*, 159. (f) Yamamoto, T. *React. Funct. Polym.* **2003**, *55*, 231.

(13) Ushiro, A.; Yamaguchi. I.; Yamamoto. T. *Annu. Meet. Chem. Soc. Jpn. (Kobe, March, 2001)* **2001**, ID208.

(14) (a) Yamamoto, T.; Kashiwazaki, A.; Kato, A. *Makromol. Chem.* **1989**, *190*, 1649. (b) Miyazaki, Y.; Yamamoto, T. *Synth. Met.* **1994**, *64*, 69. (c) Yamamoto, T.; Shiraishi, K.; Abla, M.; Yamaguchi, I.; Groenendaal, L. N.; *Polymer* **2002**, *43*, 711.

(15) (a) Yamamoto, T.; Moon, D.-K. *Makromol. Rapid Commun.* **1993**, *14*, 495. (b) Yamamoto, T. *Chem. Lett.* **1993**, 1211. (c) Kim, S.-B.; Harada, K.; Yamamoto, T. *Macromolecules* **1998**, *31*, 988.

(16) H_2O trapped by π-conjugated polymer may received unique magnetic effect. For example, the ^1H NMR signal of H_2O trapped by head-to-tail type poly(3-hexylthiophene) appears at about δ 5 (Yamamoto, T.; Komarudin, D.; Arai, M.; Lee, B.-L.; Suganuma, H.; Asakawa, N.; Inoue, Y.; Kubota, K.; Sasaki, S.; Fukuda, T.; Masuda, H. *J. Am. Chem. Soc.* **1998**, *120*, 2047), which is confirmed by H−D exchange with D_2O.

(17) Convington, A. K.; Dickinson, T. Eds.; *Physical Chemistry of Organic Solvent Systems*; Plenum: New York, 1973, p 673.

(18) Strounina, E. V.; Kane-Maguire, L. A. P.; Wallace, G. G. *Synth. Met.* **1999**, *106*, 129.

(19) Stafström, S.; Brédas, J. L.; Epstein, A. J.; Woo, H. S.; Tanner, D. B.; Huang, W. S.; MacDiarmid, A. G. *Phys. Rev. Lett.* **1987**, *59*, 1464.

(20) (a) Saprigin, A.; Kohlman, R. S.; Long, S. M.; Brenneman, K. R.; Epstein, A. J.; Angelopoulos, M.; Liao, Y.-H.; Zheng, W.; MacDiarmid, A. G. *Synth. Met.* **1997**, *84*, 767. (b) Saprigin, A. V.; Brenneman, K. R.; Lee, W. P.; Long, S. M.; Kohlman, R. S.; Epstein, A. J. *Synth. Met.* **1999**, *100*, 55.

(21) (a) Flory, P. J. *Principles of Polymer Chemistry*, Cornell University Press; Ithaca, NY, 1953. (b) Fuoss, R. M.; Strauss, U. P. *J. Polym. Sci.* **1948**, *3*, 246.

(22) Yue, J.; Epstein, A. J.; MacDiarmid, A. G. *Mol. Cryst. Liq. Cryst.* **1990**, *189*, 255.

(23) Lee, W.; Du, G.; Long, S. M.; Epstein, A. J.; Shimizu, S.; Saitoh, T.; Uzawa, M. *Synth. Met.* **1997**, *84*, 807.

(24) (a) Spindler, R.; Shriver, D. F. *J. Am. Chem. Soc.* **1988**, *110*, 1993. (b) Boino, F.; Pantaloni, S.; Passerini, S.; Scrosati, B. *J. Electrochem. Soc.* **1988**, *135*, 1961. (c) MacCallum, J. R., Vincent, C. A., Eds. *Polymer Electrolyte Review*; Elsevier: London, New York, 1989. (d) Watanabe, M.; Itoh, M.; Sanui, K.; Ogata, N. *Macromolecules* **1990**, *23*, 3118. (e) Yamamoto, T.; Inami, M.; Kanbara, T. *Chem. Mater.* **1994**, *6*, 44.

(25) Pouget, J. P.; Józefowicz, M. E.; Epstein, A. J.; Tang, X.; MacDiarmid, A. G. *Macromolecules* **1991**, *24*, 779.

(26) (a) Rietveld, H. M. *J. Appl. Crystallogr.* **1969**, *2*, 65. (b) Sasaki, S.; Yamamoto, T.; Kanbara, T.; Morita, A.; Yamamoto, T. *J. Polym. Sci., Part B: Polym. Phys. Ed.* **1992**, *30*, 293. (c) Sasaki, S.; Maehara, K.; Nurulla, I.; Yamamoto, T. *Polym. J.* **2000**, *32*, 984.

MA0209747